



Thermal-Mechanical Coupling Analysis of Track Concrete and Study on Thermal Damage at Initial Stage of Construction

Haibin Xia

Huzhou-Hangzhou Railway Co. Ltd, Hangzhou 310000, China

Corresponding Author Email: nizaijiaren@163.com

<https://doi.org/10.18280/ijht.400614>

ABSTRACT

Received: 17 September 2022

Accepted: 2 November 2022

Keywords:

track traffic project, thermal-mechanical coupling analysis, cement hydration, thermal damage model

To avoid defects in concrete structure caused by the particularity of structure, the complexity of construction process and the contingency of human operation in the track construction process, it is necessary to conduct comparative tests on the workability, strength, adiabatic and semi-adiabatic properties, free shrinkage, durability index and crack resistance of concrete before pouring. At present, in the field of track traffic, the study on establishing the thermal damage model of mass track concrete considering the thermal load is relatively lacking. The existing models do not take into account the thermal damage caused by cement hydration at the initial stage of construction of track concrete structures, and the study on thermal-mechanical coupling analysis at the initial stage of construction is also relatively rare. To this end, this article studies the thermal-mechanical coupling analysis and study on thermal damage of track concrete. It makes the thermal analysis of track concrete at the initial stage of construction by using the direct thermal-mechanical coupling analysis technology. That's, based on the updated Lagrange method, the track concrete thermal coupling equation at the initial stage of construction is constructed. Based on the damage model and direct thermal coupling analysis of track concrete, it builds a thermal damage model suitable for track concrete at the initial stage of construction. The results of thermal coupling analysis of track concrete and thermal damage mechanism analysis at the initial stage of construction are given to verify the effectiveness of the proposed analysis method.

1. INTRODUCTION

Track concrete, as the main load-bearing structural material, is also widely used in track traffic [1-6]. By virtue of its supporting, waterproof, anti-corrosion and other functions, it is widely used in structures such as shield segments, secondary lining of tunnels and main body of stations [7-11]. Concrete used in track traffic construction is often divided into two types, one is structural durability C40 concrete for ballast pouring, and the other is C30 ordinary concrete for transition section laying [12-19]. No matter which kind of concrete, its workability, strength, adiabatic and semi-adiabatic properties, free shrinkage, durability index and crack resistance shall be determined by comparative tests before pouring, in order to avoid defects in concrete structure caused by the particularity of structure, the complexity of construction process and the contingency of human operation in the track construction process [20-26]. Therefore, the study on the performance of track concrete is the hot pot and focus of safe operation of track traffic project.

Early damage of baseplate may lead to safety and durability problems of plate-type ballastless track. However, the research on the early damage mechanism of CRTS III ballastless track baseplate is very limited, which is very common in practice. Zhang et al. [27] establishes a thermal-mechanical model to study the early damage behavior of concrete in baseplate. The effects of curing method, demoulding time, demoulding temperature, steel bar diameter and longitudinal continuous

length are considered. Lee et al. [28] analyzed the performance of railway ultrahigh track system by using the railway load system built by Korea Railroad Research Institute. There are two main loading stages, including static loading and cyclic loading. A hot air purge system is installed around the bevel track to keep the temperature of the asphalt concrete core constant. On the whole, the result of full-scale test stand confirms the positive applicability of railway ultrahigh track. In order to clarify the refreezing process of bored piles, a temperature-tracked concrete hydration model is established in Gao et al. [29]. The applicability of bored piles in permafrost regions is discussed based on the initial refreezing time (IRT) of at least 30 at the pile side. The result shows that IRT increases with the increase of mean annual ground temperature (MAGT), frozen soil ice content, concrete forming temperature and pile diameter.

Any change in temperature changes the size of concrete structure and induces thermal stress. Revilla-Cuesta et al. [30] tested a reference self-compacting concrete (SCC) mixture made of 100% coarse natural aggregate and fine natural aggregate and three SCC mixtures containing 100% coarse RCA and/or fine RCA to replace natural aggregate. The mixture is subjected to five thermal tests designed for positive, negative, constant and periodic extreme ambient temperature changes up to -15°C and 70°C , respectively. The results of the tests result in a recommended linear coefficient of thermal expansion of $1.2 \cdot 10^{-5} \text{C}^{-1}$ for the calculation of SCC containing RCA under these extreme environmental

conditions. A thermal-mechanical damage model based on dimensional analysis is established in Sun [31] to describe the softening behavior of concrete materials at high temperature. The iterative process of damage renewal is coupled in the finite element method (FEM) based on modified continuous damage mechanics (CDM) to simulate the thermal damage process of concrete materials. The results show that the model and method can be used to study the thermal-mechanical behavior of concrete materials at high temperature and the calculation efficiency is high.

By combing and summarizing the existing literatures, it is found that some achievements have been made in the research of thermal fatigue and thermal expansion of track concrete considering thermal load. Experts and scholars at home and abroad have established many concrete thermal response models according to the actual situation of specific concrete application scenarios. However, in the field of track traffic, the study on establishing the thermal damage model of mass track concrete considering the thermal load is relatively lacking. The existing models do not take into account the thermal damage caused by cement hydration at the initial stage of construction of track concrete structures, and the study on thermal-mechanical coupling analysis at the initial stage of construction is also relatively rare. Therefore, the thermal-mechanical coupling analysis and study on thermal damage of track concrete are carried out in this article. In the second chapter, the direct thermal coupling analysis technology is used to carry out thermal analysis of track concrete at the initial stage of construction. That is, based on the updated Lagrange method, the track concrete thermal coupling equation at the initial stage of construction is constructed. In the third chapter, based on the damage model and direct thermal coupling analysis of track concrete, a thermal damage model suitable for track concrete at the initial stage of construction is constructed. At last, the results of thermal coupling analysis of track concrete and thermal damage mechanism analysis at the initial stage of construction are given to verify the effectiveness of the proposed analysis method.

2. DIRECT THERMAL-MECHANICAL COUPLING ANALYSIS OF TRACK CONCRETE

Thermal decoupling is the most common method in thermal coupling analysis. In this article, the direct thermal coupling analysis technology is used to carry out thermal analysis of track concrete at the initial stage of construction. That is, based on the updated Lagrange method, the track concrete thermal coupling equation at the initial stage of construction is constructed. The set shape is updated at the time of each increment based on the idea of iteration, the equivalent temperature field of concrete is deduced based on the obtained Lagrange heat conduction equation, and the related equations are obtained. Finally, the force balance equation is solved by nonlinear iteration, and if the iteration process tends to converge, the analysis of the next increment begins.

This analysis method can solve heat conduction and force balance problems of track concrete at the initial stage of construction. It is assumed that the track concrete structure analyzed at the initial stage of construction consists of a continuous medium. Its boundary is denoted by R , volume by U , velocity field by u_i , density by σ , given internal energy by V , given volume heat flow by W , given volume force by y_i , the

boundary force per unit area by e_i and the intensity of heat flow per unit area on the boundary by F , then the following energy conservation equation can be constructed:

$$\int_u \sigma u_i \frac{\partial u_i}{\partial \phi} dU + \int_u \frac{\partial \sigma}{\partial \phi} V dU = \int_u \sigma (\bar{W} + y_i u_i) dU + \int_u (e_i u_i - F) dR \quad (1)$$

An integral balance equation may also be constructed as follows:

$$\int_u \sigma \left(y_i - \frac{\partial u_i}{\partial \phi} \right) dU = \int_r e_i dR \quad (2)$$

Assuming that the Cauchy stress component is expressed by ε_{ij} and the unit normal direction of the surface R is expressed by m_i , the pressure per unit area of track concrete at the initial stage of construction is characterized based on the Cauchy stress:

$$e_i = m_i \varepsilon_{ij} \quad (3)$$

Combining Eq. (1) with Eq. (2), the energy conservation equation based on thermal coupling can be constructed as follows:

$$\int_u \left\{ \sigma \left(\bar{W} - \frac{\partial u_i}{\partial \phi} \right) + \varepsilon_{ij} \frac{\partial u_i}{\partial a_j} \right\} dU = \int_R F dR \quad (4)$$

The displacement equation of track concrete structure to be satisfied at the initial stage of construction under the virtual work principle is given as follows:

$$\int_u \varepsilon_{ij} \frac{\partial \delta v_i}{\partial a_i} dU = \int_u \sigma y_i \delta v_i dU - \int_u \sigma \frac{\partial u_i}{\partial a_i} \delta v_i dU \quad (5)$$

When the direct thermal-mechanical coupling analysis technology of Lagrange method is applied to solve the thermal-mechanical coupling problem of track concrete at the initial stage of construction, each increment needs to be analyzed based on the iteration equilibrium equation and energy conservation equation. Assuming that the stress deviator is expressed by R_{ij} , the equivalent stress is expressed by ε' , and the equivalent plastic strain is expressed by ρ' , the following equation is given to characterize the thermoelasticity of track concrete based on *Mises* yield criterion:

$$G = \frac{1}{2} R_{ij} R_{ij} - \frac{1}{3} \varepsilon'^2 (\rho'^2, O) = 0 \quad (6)$$

If the plastic strain flow during cement hydration of track concrete at the initial stage of construction should satisfy $dG=0$, then:

$$\frac{\partial G}{\partial \varepsilon_{ij}} \frac{\partial \varepsilon_{ij}}{\partial \phi} - \frac{2}{3} \varepsilon' \frac{\partial \varepsilon'}{\partial \rho'^e} - \frac{2}{3} \varepsilon' \frac{\partial \varepsilon'}{\partial O} \frac{\partial G}{\partial \phi} = 0 \quad (7)$$

The superposition of elastic strain, plastic strain and thermal strain is defined as the total incremental strain of track concrete at the initial stage of construction, and the equation is

given as follows:

$$\frac{\partial \varepsilon_{ij}}{\partial \phi} = \frac{\partial \varepsilon_{ij}^p}{\partial \phi} + \frac{\partial \varepsilon_{ij}^w}{\partial \phi} \frac{\partial \varepsilon_{ij}^e}{\partial \phi} + \frac{\partial \varepsilon_{ij}^{of}}{\partial \phi} \quad (8)$$

The following gives the equation that needs to be satisfied for materials of the same strain in different directions:

$$\varepsilon_{ij} = C_{ijkl}(O) \rho_{lk}^p \quad (9)$$

If the above two equations are combined, the equation for calculating the stress change rate of track concrete is:

$$\frac{\partial \varepsilon_{ij}}{\partial \phi} = C_{ijkl}(P) \frac{\partial \rho_{lk}^p}{\partial \phi} + \frac{\partial C_{ijkl}(O)}{\partial \phi} \frac{\partial G}{\partial \phi} \rho_{lk}^p \quad (10)$$

At the initial stage of construction, the temperature increment during the cement hydration of track concrete occurs in an extreme time and is unknown, but since the right side of the above equation is a function of temperature change rate. Therefore, the approximate value of temperature of track concrete during cement hydration can be obtained based on the method of alternating iteration. If thermal-elastic-plastic problem of large deformation appears in the cement hydration process of concrete, the thermal-mechanical coupling analysis needs to adopt the following stress change rate form. Assuming that Jaumann stress rate is represented by ε_{ij}^J and deformation rate is represented by C , then:

$$\varepsilon_{ij}^J = K_{ijkl} C_{lk} + f_{lk} O \quad (11)$$

If the track concrete structure U is known, the energy conservation equation based on thermal-mechanical coupling can be transformed into a decoupled form as follows:

$$\int_u \sigma \left(\bar{W} - \frac{CV(O)}{C\phi} \right) = \int_r F dr \quad (12)$$

Assuming that the surface heat flow during the cement hydration process of track concrete at the initial stage of construction is expressed by $w_i m_i = F$, and the outer normal direction of the surface is expressed by m_i , then:

$$\int_u \sigma \left(\bar{W} - \frac{CV(O)}{C\phi} \right) - \frac{\partial w}{\partial a_i} = 0 \quad (13)$$

If the track concrete material follows *Fourie*: heat conduction law, then:

$$w_i = -l \mu_{ij} \frac{\partial O}{\partial a_i} \quad (14)$$

Figure 1 and Figure 2 show the variation curves of thermal conductivity and specific heat of track concrete under different temperatures. As can be seen from the figures, the variation curves corresponding to different thermal conductivity formulas can all reflect the basic trend of thermal conductivity of track concrete changing with temperature, that is, the higher the temperature is, the smaller the thermal conductivity of track concrete is. The variation curves corresponding to

different specific heat formulas reflect the same change trend of specific heat of track concrete, that is, most of the specific heat calculation results increase with the rise of temperature until they tend to be stable. If the influence of elastic strain energy on the thermal conductivity of track concrete during cement hydration, there is the following temperature function expression:

$$\frac{CV}{C\phi} = \frac{CdO}{C\phi} \quad (15)$$

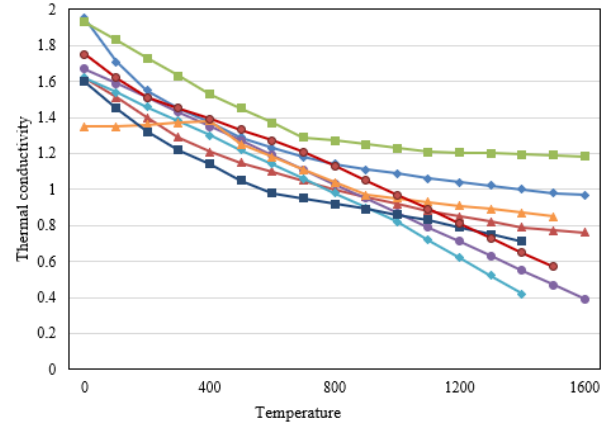


Figure 1. Variation curves of thermal conductivity of track concrete under different temperatures

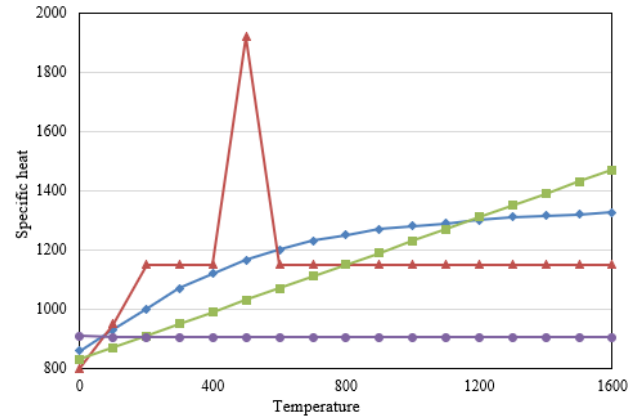


Figure 2. Variation curves of specific heat of track concrete under different temperatures

Assuming that the specific heat of concrete material is expressed by d and the Galerkin method weight function is expressed by h , the following equations give the equivalent form of solving the decoupled form of energy conservation equation by Galerkin method with weighted residuals:

$$\int_u H \sigma \bar{W} dU - \int_r h F dR = \int_u \sigma h \frac{CdO}{C\phi} dU = \int_u \frac{\partial h}{\partial a_i} l_{ij} \frac{\partial O}{\partial a_j} dU \quad (16)$$

$$\frac{CdO}{C\phi} = d \frac{\partial O}{\partial \phi} + du_i \frac{\partial O}{\partial a_i} \quad (17)$$

When calculating the temperature field of track concrete in the process of cement hydration, it is assumed that the plastic power is expressed by $\partial Q_e / \partial \phi$, and the proportion of plastic work converted into heat flow in the whole plastic work is

expressed by g , the following equation gives the heat-enthalpy expression converted into plastic dissipation work of track concrete:

$$O \frac{\partial R}{\partial \phi} = g \frac{\partial Q^E}{\partial \phi} \quad (18)$$

The surface heat flow generated by plastic work of track concrete is converted into volume heat flow, then:

$$W = Ng \frac{\partial Q^E}{\partial \phi} \quad (19)$$

3. ESTABLISHMENT OF THERMAL DAMAGE MODEL OF TRACK CONCRETE

Because of the hydration of cement, the variable temperature load, which rises first and then cools down, is the main reason for the damage of track concrete structure at the initial stage of construction. At present, there are few thermal damage models of track concrete that can be used in engineering practice. Based on the analysis results of damage model and direct thermal-mechanical coupling of track concrete, this article builds a thermal damage model of track concrete suitable for initial construction.

It is very difficult to measure and quantify the damage degree of damaged concrete materials in practice. Only by using the strain equivalence principle to measure indirectly can we get more accurate quantitative results. In this article, the concept of effective stress is introduced into the study of elastic deformation mechanism of damaged track concrete materials at the initial stage of construction, and it is applied to the elastic strain ρ and equivalent stress ε of concrete materials.

The strain produced by default equivalent stress ε acting on damaged track concrete at the initial stage of construction is equal to the strain produced by effective stress acting on nondestructive track concrete. Assuming that the elastic modulus of damaged track concrete material is expressed by $P=(1-C)P$, then:

$$\rho = \frac{\varepsilon}{P} = \frac{\varepsilon}{(1-C)P} \quad (20)$$

$$\varepsilon = (1-C)O\rho \quad (21)$$

The constitutive relation of damaged track concrete material in one-dimensional problem is revealed by the above formula. The elastic modulus is satisfied by P :

$$C = 1 - \frac{P}{P_0} \quad (22)$$

If $\varepsilon=(1-C)P\rho$ is differentiated, then:

$$\frac{d\varepsilon}{d\rho} = \frac{dP}{d\rho}(1-C)\rho + P(1-C) - P\rho \frac{dC}{d\rho} \quad (23)$$

In the process of thermal damage test of track concrete, the load is removed immediately after the increased load reaches

the preset threshold, and the thermal damage of track concrete during the loading-removing process is completely irreversible by default, then $dC/d\rho=0$, which meets the following requirements:

$$\frac{d\varepsilon}{d\rho} = (1-C)P \quad (24)$$

$$C = 1 - \frac{1}{P} \frac{d\varepsilon}{d\rho} \quad (25)$$

In combination with Formula 20, then:

$$P = \frac{d\varepsilon}{d\rho} \quad (26)$$

From the above analysis, it can be seen that the stress-strain ratio of damaged track concrete when the load is removed represents its elastic modulus P . Therefore, the size of P can be determined by the tensile loading-unloading test of track concrete, and the damage variable C of track concrete can be further obtained. Or the analytic curve of $\varepsilon-\rho$ is further drawn from the measured $\varepsilon-\rho$ relationship curve; then P is obtained based on $d\varepsilon/d\rho$, and C is further obtained.

P in the damage evolution equation of track concrete mentioned above is equivalent strain, so in theory ε is the comprehensive superposition ρ_{TOTAL} under various loads in the damage evolution process, including dead loads such as concrete deadweight, earth pressure and prestress; live loads such as temperature load, crane load, wind load and snow load; accidental loads such as earthquake and impact force. The ρ_{TOTAL} expression is as follows:

$$\rho_{TOTAL} = \rho_{ST} + \rho_{CH} + \rho_{AC} \quad (27)$$

According to the above formula, in the damage evolution analysis of track concrete, it is only necessary to obtain a certain strain at a certain position of the track concrete at a certain time for the quantitative value of the damage at that position through deduction. This way of solving the problem of quantifying the damage degree by constructing the relationship between material strain and damage in the process of damage evolution of track concrete is not only simple in calculation, but also has practical and reliable theoretical basis as well as high practical application value.

The research object of this article is the thermal damage of track concrete, so this article only considers the temperature load of track concrete structure, that's, $\rho_{ST}=\rho_{AC}=0$, $\rho_{CH}=\rho_O$, so according to the above formula, it can be obtained:

$$\rho_{TOTAL} = \rho_{CH} = \rho_O \quad (28)$$

Based on ρ_{TOTAL} , the thermal damage model of track concrete based on exponential function is constructed, and the model expression is given by the following formula:

$$C = \begin{cases} C_0 + \frac{\rho_O}{\rho_g}(C_g - C_0); (\rho \leq \rho_g) \\ 1 - (1 - C_g) \left\{ p^{-\left(\frac{\rho_O - \rho_g}{\rho_v - \rho_g}\right)^2 g(\rho_O)} - \left(\frac{\rho_O - \rho_g}{\rho_v - \rho_g}\right) p^{-g(\rho_O)} \right\}; (\rho > \rho_g) \end{cases} \quad (29)$$

$$g(\rho_O) = Y * \left(\frac{\rho_O - \rho_g}{\rho_v - \rho_g} \right)^D$$

4. TEST RESULTS AND ANALYSIS

Two kinds of concrete are used for the track concrete samples tested in this article, one is structural durability C40 concrete used for ballast pouring, and the other is C30 ordinary concrete used for foundation of transition section. Table 1 gives the test results of compressive strength of concrete specimens. It can be seen from the table that with the increase of temperature, the compressive strength of the two kinds of track concrete decreases first and then increases, which is because the outside temperature is too low at first, which can't make the track concrete lose its strength, but accelerates the hydration speed of track concrete cement. Until the high temperature can destroy the structure of concrete, it will lead to temperature deformation and internal and external stress between aggregate and cement slurry in concrete, which will accelerate the development of thermal damage of concrete. Figure 3 shows the curves of compressive strength of concrete specimens under different temperature conditions.

Table 1. Test results of compressive strength of concrete specimens

Concrete type	Specimen No.	Compressive strength	Strength discount rate
C40	C40-1	46.4	1
	C40-2	49.3	1.062
	C40-3	42.8	0.925
	C40-4	29.5	0.634
	C40-5	46.6	0.996
C30	C30-1	44.8	0.971
	C30-2	38.6	0.834
	C30-3	27.3	0.588
	C30-4	45.1	0.974

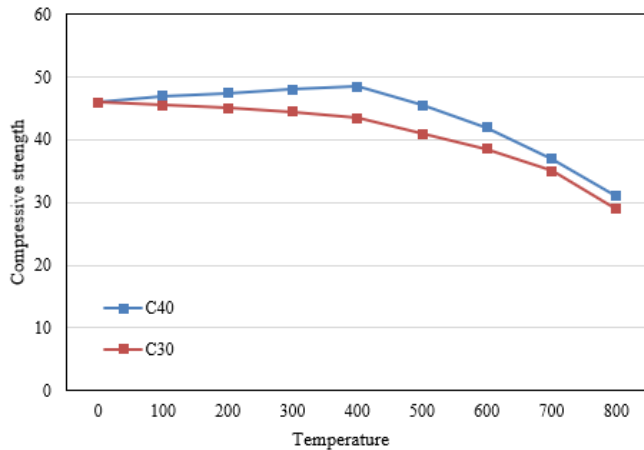


Figure 3. Variation curves of compressive strength of concrete specimens under different temperature conditions

The tensile strength of track concrete is the key factor to the thermal damage of concrete under thermal stress. Table 2 gives the test results of tensile strength of concrete specimens. It can be seen from the table that the tensile strength of track concrete which is more affected by temperature does not decrease first and then increase with the increase of temperature, which is mainly due to the different causes of concrete damage under compressive and tensile tests. Different from compressive test, it's easier to further develop the surface damage of high temperature track concrete under concentrated load of cushion blocks at both ends. In order to

reduce the sudden change in temperature caused by cement hydration of track concrete, cold air treatment is carried out in this article. The increase in damage quantity of uncooled concrete specimens is always below that of cooled concrete specimens, and the higher the temperature is, the more obvious the difference of damage quantity is. The results of compressive and tensile tests are basically consistent, which is also consistent with the conclusions given in other references. Figure 4 shows the variation curves of tensile strength of concrete specimens under different temperature conditions.

Table 2. Test results of tensile strength of concrete specimens

Concrete type	Specimen No.	Tensile strength	Strength discount rate
C40	C40-1	398	1
	C40-2	3.12	0.778
	C40-3	2.15	0.534
	C40-4	1.56	0.387
	C40-5	2.93	0.726
C30	C30-1	2.94	0.735
	C30-2	1.86	0.453
	C30-3	0.97	0.242
	C30-4	2.68	0.668

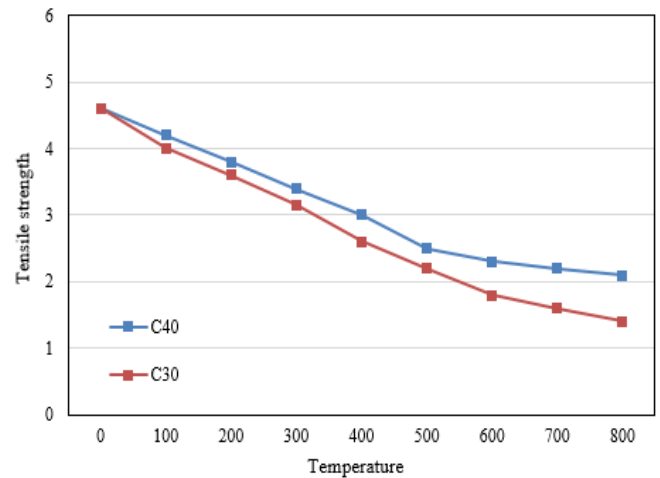


Figure 4. Variation curves of tensile strength of concrete specimens under different temperature conditions

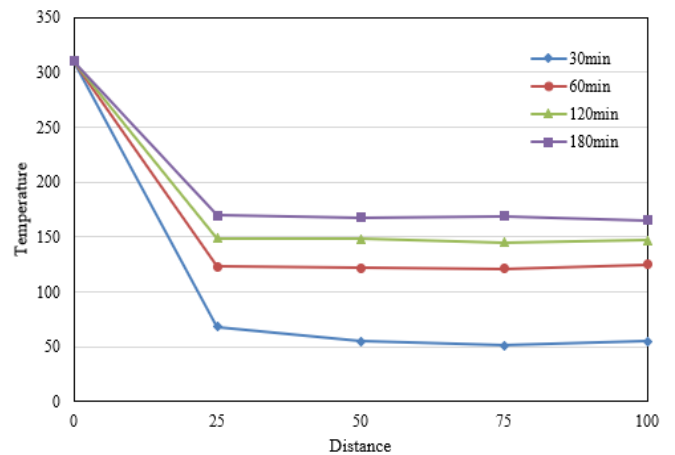


Figure 5. Cross-section temperature field of 300°C high temperature track concrete specimens

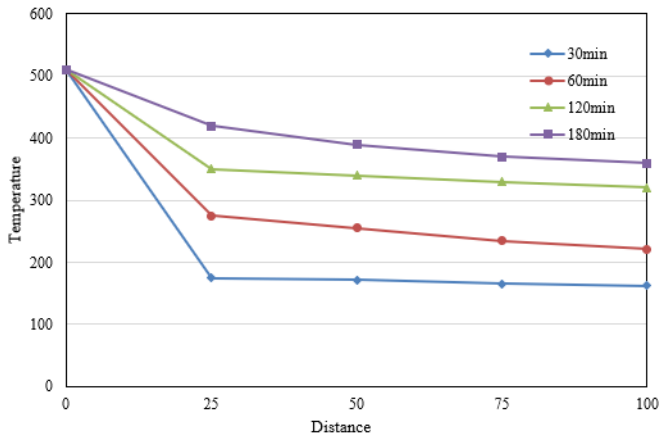


Figure 6. Cross-section temperature field of 500°C high temperature track concrete specimens

Figures 5 and 6 show the temperature distribution at different measuring points of 300°C high temperature track concrete specimen section. The concrete position distributes in the track concrete cover, the cross-section symmetry axis and the area between the cover and the symmetry axis, and the distribution position is relatively uniform. As can be seen from Figures 5 and 6, the temperature inward from the track concrete surface decreases in turn along its cross-sectional width and height direction, and the closer to the surface, the greater the temperature difference between measuring points is. The change trend of broken lines corresponding to different initial construction periods is first reduced and then tends to be flat, which shows that the temperature rises rate of measuring points closer to the track concrete surface is faster, which is basically consistent with the previous analysis. Based on the temperature field distribution of the specimen interface and the mechanical properties of the track concrete at the initial stage of construction, the residual bearing capacity of the track concrete at the initial stage of construction at high temperature can be further calculated, and the high temperature resistance limit of the track concrete can be estimated.

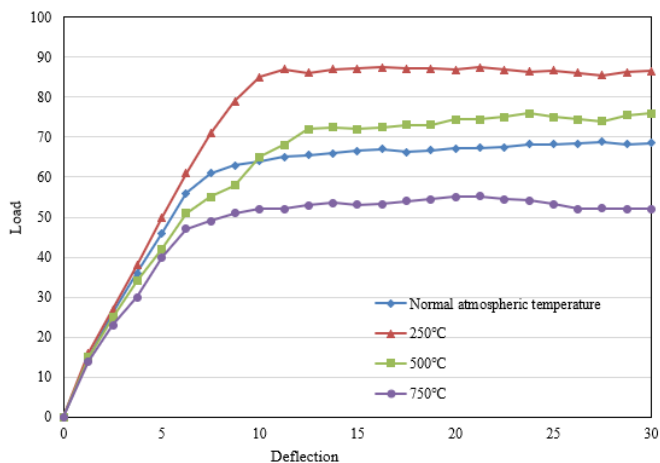


Figure 7. Deflection curve of concrete specimen under flexural load

Figure 7 shows the deflection curve of concrete specimen under flexural load. Combined with the failure process of track concrete, this article compares the load-deflection curves of various specimens under different temperature conditions, which shows that the evolution law of damage degree and deflection is basically consistent, but there are also differences

under different temperature conditions. The load-deflection curve of track concrete shows a straight upward trend before the damage occurs, and the curve shows obvious rotation angle when the damage occurs, which shows that the stiffness of track concrete decreases after the damage occurs. After high temperature, the track concrete is damaged seriously, and the damage develops rapidly, and the number is increasing cumulatively. During the construction period, the track concrete appears thermal damage earlier, which makes it difficult to bear greater load.

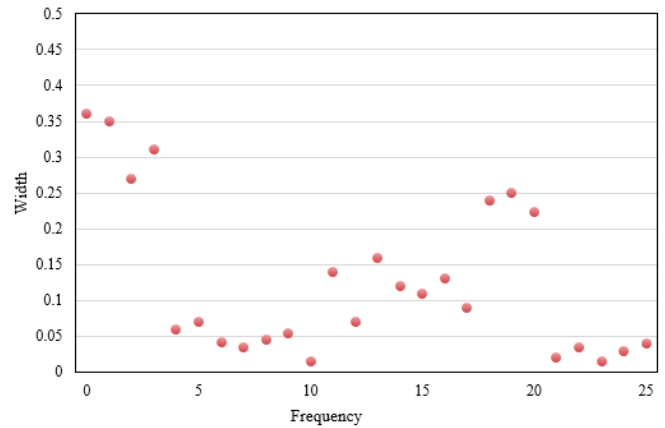


Figure 8. Damage width data of track concrete at 300°C

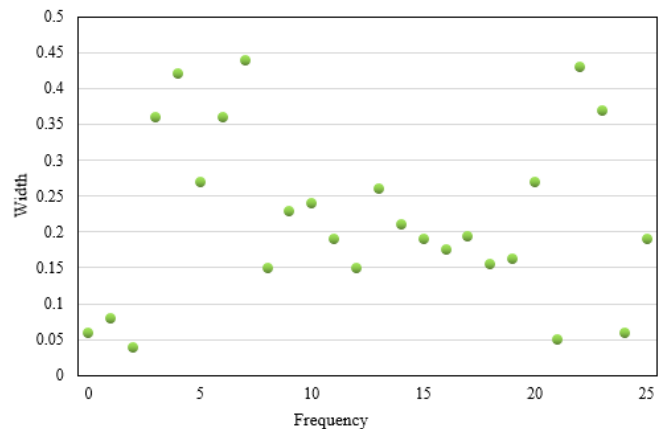


Figure 9. Damage width data of track concrete at 500°C

This article experimentally counts the pure temperature damage width data of track concrete, and the specific statistical results are given in Figures 8 and 9. It can be seen from the figures that there is a certain regularity in the thermal damage width of track concrete after high temperature. The damage width is between 0.025 mm-0.095 mm at 300°C and between 0.175 mm-0.260 mm at 500°C, and the thermal damage tends to be serious.

In the process of heating test, the track concrete specimens appear several bursts, with certain laws in bursting temperature, bursting time, bursting duration, bursting damage form, etc. Table 3 gives the occurrence and evolution law of bursting damage.

It can be seen from the table that the track concrete specimens are prone to burst at about 500°C, and the burst usually occurs in about 30 minutes and lasts for about 20 minutes at the heating rate of 12°C/min-13°C/min. It is mainly caused by the difference of temperature rise rate and cement hydration cooling mode.

Table 3. Occurrence and evolution of burst damage

Test temperature	Frequency	Bursting temperature	Bursting time	Bursting duration	Maximum volume failure rate
500°C	4	445	30.9	23.9	35%
700°C	4	509	35.7	4.5	43%
900°C	2	432	29.6	-	24%

5. CONCLUSION

This article studies the thermal-mechanical coupling analysis and study on thermal damage of track concrete. It makes the thermal analysis of track concrete at the initial stage of construction by using the direct thermal-mechanical coupling analysis technology. That's, based on the updated Lagrange method, the track concrete thermal coupling equation at the initial stage of construction is constructed. Based on the damage model and direct thermal coupling analysis of track concrete, it builds a thermal damage model suitable for track concrete at the initial stage of construction. It carries out the compressive and tensile tests of track concrete specimens, gives the experimental analysis results, and draws the curves of compressive strength and tensile strength of concrete specimens under different temperature conditions. It shows the temperature distribution at different measuring points in the section of 300°C high temperature track concrete specimens, and delivers the estimation idea of high temperature resistance limit of track concrete. It develops the deflection curve of concrete specimens subjected to flexural load and counts the pure temperature damage width data of track concrete, verifying that the thermal damage width of track concrete after high temperature has certain regularity. Finally, it concludes the occurrence and evolution laws of burst damage, and analyzes the main causes of bursting.

REFERENCES

- [1] Cho, Y.K., Kim, S.M. (2018). Evaluation of grouting layer vibration of railway precast concrete slab track system. *Construction and Building Materials*, 193: 244-254. <https://doi.org/10.1016/j.conbuildmat.2018.10.216>
- [2] Liu, X., Yu, Z., Xiang, P., Jin, C. (2019). Composite action of the track slab and the self-compacting concrete filling layer subjected to train-induced fatigue load: An experimental investigation. *Proceedings of the Institution of Mechanical Engineers, Part F: Journal of Rail and Rapid Transit*, 233(5): 580-592. <https://doi.org/10.1177/0954409718803821>
- [3] Lee, S.H., Park, D.W., Vo, H.V., Fang, M. (2019). Analysis of asphalt concrete track based on service line test results. *Construction and Building Materials*, 203: 558-566. <https://doi.org/10.1016/j.conbuildmat.2019.01.131>
- [4] Liu, K.W., Yue, F., Su, Q., Liu, B., Zhou, P. (2019). Investigation of concrete base-roadbed surface contact variation-induced vibration characteristics of vehicle-slab track-subgrade system considering fluid-solid interaction. *Shock and Vibration*, 2019: 1570736. <https://doi.org/10.1155/2019/1570736>
- [5] Cai, D., Chen, P., Shi, Y., Yao, J., Yan, H., Peng, P. (2022). Analytical calculation method for passive tensile damage of asphalt concrete waterproof sealing structure of ballastless track subgrade. *Construction and Building Materials*, 320: 126158. <https://doi.org/10.1016/j.conbuildmat.2021.126158>
- [6] Ge, X., Tan, Y., Wang, X., Xie, Y., Li, Q., Li, L., Feng, Z. (2022). Research on water absorption and frost resistance of concrete coated with different impregnating agents for ballastless track structure. 7 th International Conference on the Durability of Concrete Structures, University of Jinan, Jinan, Shandong, China, pp. 1-4.
- [7] Liu, G., Qian, Z., Yang, D., Liu, Y., Yin, Y. (2022). Investigation of asphalt concrete used as the ballastless track substructure in long-span railway bridges. *Case Studies in Construction Materials*, 17: e01396. <https://doi.org/10.1016/j.cscm.2022.e01396>
- [8] Yastremsky, D., Abaidullina, T., Chepur, P. (2018). Statistical test data evaluation of track rutting in stone mastic asphaltic concrete. In: Murgul, V., Popovic, Z. (eds) *International Scientific Conference Energy Management of Municipal Transportation Facilities and Transport EMMFT 2017*. EMMFT 2017. *Advances in Intelligent Systems and Computing*, vol 692. Springer, Cham. https://doi.org/10.1007/978-3-319-70987-1_106
- [9] Mirza, O., Kaewunruen, S. (2018). Influence of shear bolt connections on modular precast steel-concrete composites for track support structures. *Steel Comp. Struct*, 27: 647-659.
- [10] Kazanskaya, L., Smirnova, O. (2020). Influence of mixture composition on fresh concrete workability for ballastless track slabs. In *E3S Web of Conferences*, 157: 06022. <https://doi.org/10.1051/e3sconf/202015706022>
- [11] Ahmed, S., Atef, H., Husain, M. (2022). Improvement of mechanical properties of railway track concrete sleepers using ultra high performance concrete (UHPC). *Frattura e Integrita Strutturale*, (60).
- [12] Ye, Y.S., Lou, L.W., Cai, D.G., Shi, Y.F., Yan, H.Y., Wei, S.W. (2022). Mechanical properties of track-asphalt concrete-subgrade bed structure system under both temperature and train loading. *Construction and Building Materials*, 340: 127556. <https://doi.org/10.1016/j.conbuildmat.2022.127556>
- [13] Li, X., Ren, J., Wang, J., Yang, R., Shi, L., Liu, X. (2020). Drying shrinkage of early-age concrete for twin-block slab track. *Construction and Building Materials*, 243: 118237. <https://doi.org/10.1016/j.conbuildmat.2020.118237>
- [14] Rozli, M.I.F., Safiuddin, C.M.C.J.M.H., Harun, M., Ahmad, J., Amin, N.M., Dora, A.K. (2019). The behaviour of Prestressed Concrete Sleeper (pcs) sitting on railway track. In *IOP Conference Series: Materials Science and Engineering*, 615(1): 012123. <https://doi.org/10.1088/1757-899X/615/1/012123>
- [15] Peng, H., Zhang, Y., Wang, J., Liu, Y., Gao, L. (2019). Interfacial bonding strength between cement asphalt mortar and concrete in slab track. *Journal of Materials in Civil Engineering*, 31(7): 04019107.
- [16] Cho, Y.K., Kim, S.M. (2019). Experimental analysis of crack width movement of continuously reinforced concrete railway track. *Engineering Structures*, 194: 262-273. <https://doi.org/10.1016/j.engstruct.2019.05.075>

- [17] Izvolt, L., Dobes, P., Mekar, M. (2019). Testing the suitability of the reinforced foam concrete layer application in the track bed structure. In IOP Conference Series: Materials Science and Engineering, 661(1): 012014. <https://doi.org/10.1088/1757-899X/661/1/012014>
- [18] Watanabe, T., Goto, K., Matsuoka, K., Minoura, S. (2020). Validation of a dynamic wheel load factor and the influence of various track irregularities on the dynamic response of prestressed concrete sleepers. Proceedings of the Institution of Mechanical Engineers, Part F: Journal of Rail and Rapid Transit, 234(10): 1275-1284. <https://doi.org/10.1177/095440971989165>
- [19] Zheng, Z., Liu, P., Yu, Z., Kuang, Y., Liu, L., He, S., Zhnag, X., Li, Q., Xu, W., Lv, M. (2022). Numerical investigation of interlaminar stress of CRTS II slab ballastless track induced by creep and shrinkage of concrete. Materials, 15(7): 2480. <https://doi.org/10.3390/ma15072480>
- [20] Bhardwaj, S., Patel, Y., Rastogi, V. (2022). Bond graph analysis of dynamic interaction between the concrete slab and subgrade for high-speed track. In: Popuri, B., Tyagi, A., Chauhan, N.R., Gupta, A. (eds) Recent Trends in Engineering Design. Lecture Notes in Mechanical Engineering. Springer, Singapore. https://doi.org/10.1007/978-981-16-2900-6_1
- [21] Su, M., Dai, G., Peng, H. (2020). Bond-slip constitutive model of concrete to cement-asphalt mortar interface for slab track structure. Struct. Eng. Mech, 74(5): 589-600. <https://doi.org/10.12989/sem.2020.74.5.589>
- [22] Zhang, J., Zhu, S., Cai, C., Wang, M., Li, H. (2020). Experimental and numerical analysis on concrete interface damage of ballastless track using different cohesive models. Construction and Building Materials, 263: 120859. <https://doi.org/10.1016/j.conbuildmat.2020.120859>
- [23] Niedostatkiewicz, M. (2018). Degradation of the concrete railway track bed located in the vicinity of the loading wharf. Polish Maritime Research, 25(4): 149-153. <https://doi.org/10.2478/pomr-2018-0141>
- [24] Lee, S.C., Park, S., Lee, J., Lee, K.C. (2018). Dowel behavior of rebars in small concrete block for sliding slab track on railway bridges. Advances in Materials Science and Engineering, 2018: 3182419. <https://doi.org/10.1155/2018/3182419>
- [25] Markul, R.V., Hubar, O.V., Arbuzov, M.A., Andrieiev, V.S., Tiutkin, O.L., Savyts'ky, V., Ganich, R.P. (2020). Investigation of the operation of the railway track with reinforced concrete sleepers in curved sections with radius $R \leq 350$ m. Proceedings of 24th International Scientific Conference. Transport Means 2020, pp. 520-527.
- [26] Ramos, Ó.R., Schanack, F., Carreras, G.O., de Vena Retuerto, J. (2019). Bridge length limits due to track-structure interaction in continuous girder prestressed concrete bridges. Engineering Structures, 196: 109310. <https://doi.org/10.1016/j.engstruct.2019.109310>
- [27] Zhang, K., Yuan, Q., Huang, T., Zuo, S., Chen, R., Wang, M. (2022). Predicting the cracking behavior of early-age concrete in CRTS III track. Construction and Building Materials, 353: 129105. <https://doi.org/10.1016/j.conbuildmat.2022.129105>
- [28] Lee, S.H., Choi, C.Y., Le, T.H.M., Park, D.W. (2023). Full-Scale investigation on inclined ballastless cant track using concrete slab panel at high temperature setting. Construction and Building Materials, 366: 130225. <https://doi.org/10.1016/j.conbuildmat.2022.130225>
- [29] Gao, Q., Wen, Z., Ming, F., Liu, J., Zhang, M., Wei, Y. (2019). Applicability evaluation of cast-in-place bored pile in permafrost regions based on a temperature-tracking concrete hydration model. Applied Thermal Engineering, 149: 484-491. <https://doi.org/10.1016/j.applthermaleng.2018.12.097>
- [30] Revilla-Cuesta, V., Skaf, M., Santamaría, A., Espinosa, A.B., Ortega-López, V. (2022). Self-compacting concrete with recycled concrete aggregate subjected to alternating-sign temperature variations: Thermal strain and damage. Case Studies in Construction Materials, 17: e01204. <https://doi.org/10.1016/j.cscm.2022.e01204>
- [31] Sun, B. (2022). A dimensional analysis based thermal-mechanical damage model for crack growth simulation of concrete-like materials at elevated temperatures. Construction and Building Materials, 357: 129429. <https://doi.org/10.1016/j.conbuildmat.2022.129429>